Journal of Ovonic Research Vol. 21, No. 1, January - February 2025, p. 29 - 35

Synthesis and characterization of ZnO QDs - GO core-shell nanoparticles via sonochemistry

A. J. López Ramírez [a], A. I. Díaz Cano [a,*], A. García Murillo [b]
[a] *Instituto Politécnico Nacional - UPIITA, México*
[b] *Instituto Politécnico Nacional - CIITEC, México*

In this work, an innovative approach for the synthesis of ZnO QDs-GO core-shell nanostructures by ultrasonic bath sonochemistry is presented. This method allows the formation of nanostructures with a ZnO QDs core and outer layer of GO sheets, optimizing the formation and interaction. The proposed concentration conditions of the precursors achieve morphological control and structural properties of the nanostructures. The characterizations carried out by FT-IR, Raman and TEM confirm the successful formation of the CS structure. This work provides a significant advance in the compression and control of formation of nanohybrid structures, redesigning the synthesis for various technologies.

(Received November 5, 2024; Accepted January 10, 2025)

Keywords: ZnO QDs, GO, Core-shell

1. Introduction

Core-shell (CS) hybrid nanostructures can be classified by considering two or more materials in multiple layers around a core of different material or materials. They can be classified as organic, inorganic or a combination of both; for example, the quantity and quality of CS are dependent on the medium, the shell and its thickness modify the properties of the nanoparticle. CS have many advantages including multiple combinations with materials and precursors, this adaptability allows for a wide range of applications and opens new possibilities in nanotechnology [1, 2].

ZnO quantum dots (ZnO QDs) are considered to be group II-VI semiconductors and have been widely used as light emitting diodes because of their wide bandgap (around 3.3 eV) and high exciton binding energy (~60 meV at room temperature). In the case of ZnO, it has been determined that the Bohr radius of the exciton is minimal, <3.6 nm [3, 4]. These particles are confined in the three spatial dimensions. There are different synthesis methods, such as Sol-Gel, hydrothermal and ultrasonic. One technique used is that of Spanhel & Anderson [5, 6] wich is used for the synthesis of the colloidal solution of ZnO quantum dots, which presents qualities such as good biocompatibility, physicochemical stability, imaging, antibacterial and antifungal and low cost [7].

Graphene, on the other hand, graphene is a novel material; consists of hexagonal arrangement of carbon atoms of a honeycomb network with a carbon atom at each vertex: its different properties are due to its allotropic form as well as 3D graphitic form, graphene (2D), nanotubes (1D) and reaching quantum dots (QD). Graphene oxide (GO) is a two-dimensional material with C-O covalent bond, widely used for its properties, applications and chemical functionalization. The non-stoichiometric formula is CxHyOz [9, 10]; where the hydroxyl and epoxide groups are located on the surface of the GO layer and the ionizable groups are on the edges of the GO sheet [8-10]. Wrapping ZnO quantum dots in graphene oxide improves dispersibility in solutions, enhances photocatalytic efficiency the GO is an electron acceptor facilitating the separation of the photoexcited electron-hole pairs produced in ZnO, increases surface area, improves stability and introduces opportunities for further functionalization. These combined properties make GO-ZnO composites highly effective in a variety of advanced applications, as environmental remediation, sensors, energy storage, and optoelectronic devices.

The use of ultrasonic frequencies (greater than 20 kHz) passing through the medium produces chemical reactions and cavitation processes involving the creation, expansion of bubbles

---

[*] Corresponding author: aidiaz@ipn.mx

https://doi.org/10.15251/JOR.2025.211.29

and finally implosive collapse in the fluid. Bubble collapse occurs at different locations in liquid media, leading to the creation of supercritical environments as high pressure around1000 atm and high temperature around 5000 K; this is known as sonochemistry [11].

In the case of sonication-assisted liquid phase exfoliation (LPE) is suitable solvents are selected to create conditions that support the formation of stable dispersions. and minimizing the area of contact surfaces between solvent-graphene interaction during sonication such as organic solvents like DMSO [12]. Van der Waals type π - π interactions occur between graphene layers maintained at a stacking distance of 3.35 to 0.34 Å. The surface tension of the solvent that can exfoliate graphene is 30 to 40 mJ m^{-2} because it can minimize the interfacial tension between graphene and solvent [13, 14]. several researches exist in the literature that talk about the preparation of ZnO-GO CS, with methods such as mechano-chemical, hydrothermal and even sonochemical by tip. It is important to synthesize ZnO-GO CS-type nanostructures due to the combination of new properties and a significant impact in multiple scientific areas, this work focuses on the study of the properties of GO-ZnO CS obtained from a technique such as sonochemical synthesis in an ultrasound bath, which is a simple, low-cost and novel method in which, in this article, the formation mechanism of the CS will be discussed along with the new properties of this nanostructure.

2. Experimental

Analytic-grade chemical reagents were used to synthesize the materials graphite powder from a pencil manufacturer. Sulfuric acid (H_2SO_4) and sodium nitrate ($NaNO_3$), nitric acid (HNO_3), dimethyl sulfoxide (DMSO), and ethylene glycol were purchased from J.T. Baker (>99 wt% purity), hydrogen peroxide (H_2O_2), and potassium permanganate ($KMnO_4$) (Meyer). lithium hydroxide monohydrate ($LiOH{\cdot}H_2O$) and Zinc acetate dihydrate ($Zn(CH_3COO)_2 \cdot 2H_2O$), heptane ($C_7H_{16}$) (Aldrich) (>99 wt% purity).

The methodology consists of carrying out 3 chemical synthesis processes consisting of obtaining QDZnO on the other hand GO synthesis and once these two nanomaterials were obtained the next process is synthesize GO-ZnO CS described below (Fig. 1)

2.1. Synthesis of GO

GO was synthesized through a modified version of the Hummers method. (MHM); 1 g of pencil graphite powder with 50 ml of H_2SO_4.and 0.5 g of $NaNO_3$ After that, the mixture was stirred vigorously for 1 h. After, the solution was cooled with an ice bath with stirring, and simultaneously, $KMnO_4$ (3 g) was slowly added and stirred for 30 minutes. Once this stage was concluded, 10 ml HNO_3 was slowly added dropwise and the stirring continued for 1 h. Then, it was purified by filtration using a 5 μm filter and washing with deionized water to obtain a dark-colored tablet. This was placed in a glass and left to dry in an oven at 85 °C for 24 h to eliminate excess moisture.

2.2. Synthesis of ZnO QDs

ZnO QDs were synthesized by Spanhel and Anderson's method. A 5 mmol sample of Zinc acetate dihydrate ($Zn(CH_3COO)_2 \cdot 2H_2O$) was dissolved in 50 mL ethanol at 80 °Cand then cooled quickly in ice. On the other hand, 7 mmol of $LiOH{*}H_2O$ and 50 mL of ethanol was dissolved in in an ultrasonic bath and then cooled. The last solution was added dropwise by titration to the $Zn(CH_3COO)_2 \cdot 2H_2O$ solution and stirring until the $LiOH{*}H_2O$ solution in 50 mL of ethanol was finished.

2.3. Synthesis of ZnO-GO Core-Shell

The CS nanocomposite of ZnO-GO is produced by ultrasound. GO was added to DMSO at a concentration of 2.9 mmol and sonicated for 1 h and 10 mL of ZnO QD was dissolved in the solution and sonicated for 20 min. Then, 30 mL of EG and 1 mL of SDS were added and sonicated for 2 h.

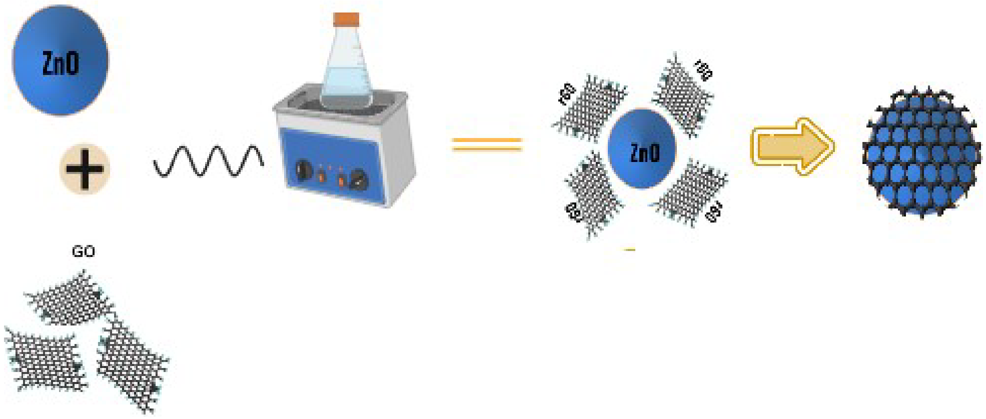

Fig. 1. Schema of synthesis of CS synthesis by sonochemical.

3. Methods

Infrared FTIR analyses were carried out using a Perkin-Elmer Frontier FTIR spectrometer in a spectral range from 4000 to 800 cm^{-1}. Micrographs were obtained by a High- Resolution Transmission Electron Microscope (HRTM) Jeol JEM 2100. The Raman spectra were using micro-Raman with an excitation length of 532 nm with a Jobin Yvon HR800 LabRam spectrometer (Horiba Ltd., Tokyo, Japan) coupled with an Olympus BX4 confocal microscope at room temperature from samples deposited on Si wafers.

4. Results and discussion

4.1. FT-IR

The ZnO QDs was subjected to FTIR analysis to find functional groups present in these nanoparticles. In Fig. 2a, the absorption peaks in the graph correspond to the positions of the interactions of the vibrational modes. A broad spectrum at 3330 and 3000 cm^{-1} represents the stretching of hydroxyl groups. The absorption band at 1634 cm^{-1} show evidence of C=C stretching type vibrational mode. An absorption band at 1033 cm^{-1}, it is due to the in-plane C– H bending. The peaks at 701 and 575 cm^{-1} confirm the presence of the metal- oxygen Zn-O. For the characterization of the GO sheets, functional groups are observed in Fig. 2b; the band at 3338 cm^{-1} is due to O-H stretching. The 2980 to 2800 cm^{-1} peaks are attributed to sp^3 symmetric and asymmetric C stretching-type bands. This may occur due to non-specific adhesion of carbon on the active surface. The peak at 1653 cm^{-1} is to the C=O functional group; at 1403 cm^{-1} and 1042 cm^{-1} was presented for C-O stretching type vibrational mode. The peaks at 1083 to 1060 cm^{-1} on the surface of the GO sheets [15]. In the band at 1718 cm^{-1}, carbonyl bonds (C=O) are present. In the band around 1179 cm^{-1}, the carbon-hydroxyl group (C- OH) bonds are present.

In the case of the CS in Fig. 2c, it presents a stretching absorption band at 3339 and 3442 cm^{-1} of the hydroxyl O-H functional groups, from 2953-2875 cm^{-1} the C-H group is present as a tension vibration (symmetric and asymmetric). At 1670 cm^{-1}, show the presence of the C=C stretching type vibrational mode also at 1424 cm^{-1}, the deformation vibrational mode of the C=O group, and at 1218 cm^{-1}, the antisymmetric vibrational mode C-O-C and from 1090 to 991 cm^{-1}, the symmetric and asymmetric vibrational mode of the C-O group. These last 4 groups are typical of GO, interacting due to the deformation produced on the surface of the CS.

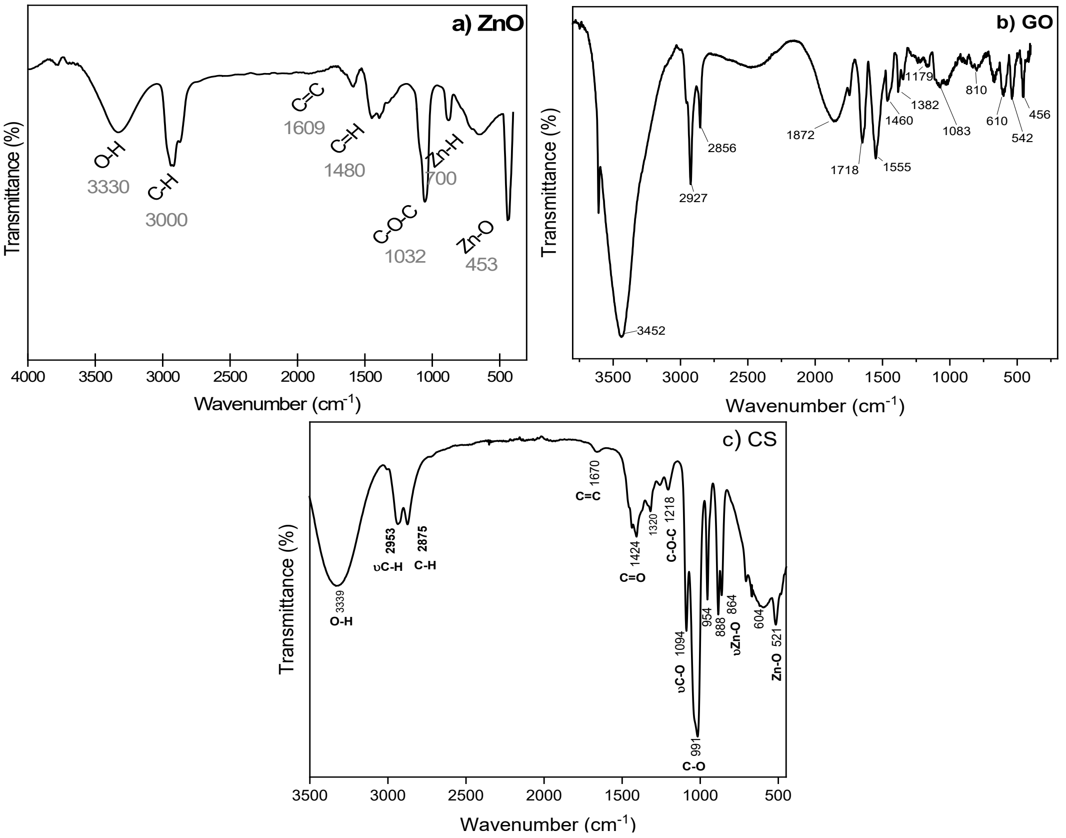

Fig. 2. FT-IR spectra of a) ZnO QDs, b) GO, and c) CS.

4.2. Raman

Raman spectra of the synthesized of ZnO QDs, GO and ZnO CS nanohybrids covered with GO films as shown in Fig. 4. The ZnO QDs were excited at wavelength of 325 nm, the spectra has been found two phonon modes of Longitudinal optical (LO) and transverse optical (TO) modes are categorized further into A1 and E1 symmetry groups. as shown in Fig. 3c. Also, the called low-frequency E2 mode is correlated to the mode of vibration of Zn ion lattice and the high-frequency E2 mode is associated with the mode vibration of oxygen ion, all these peaks are below 1LO. Subsequently, it occurs at 2LO (943 cm^{-1}) and 3 LO (1435 cm^{-1}) [14], besides presenting the B^{Low} and B^{high} modes at 269 cm^{-1} and 508 cm^{-1} respectively[13], [16]. So, the wurtzite ZnO structure of lattice optical phonon at the center of the Brillouin zone, $\Gamma = A1 + 2B1 + E1 + E2$[17].

In the case of GO, the Raman spectra spans from 1000 to 3300 cm^{-1}; in Fig. 3b, two leading bands are shown formed by the Stokes phonon energy shift. The first D peak is related to phonon dispersion (1340 cm^{-1}) and corresponds to the sp^2 mode due to the disordered oxygen bonding groups. The second notable peak, known as the G peak, located around 1595 cm^{-1} and originates from the in-plane vibration of the E2g phonon and the sp^2 hybridization, in-plane stretching vibration of the carbon atoms, that peak corresponds at the first-order dispersion of E2g in the Γ point reflecting the stretching of C–C bond in graphitic materials.

When studying the different shifts of the Raman spectra of the CS Fig. 3a, the D (1348 cm^{-1}) and G bands are present the double peak of the G^- band (1568 cm^{-1}) and the G^+ band (1600 cm^{-1}) can be attributed to the bending that comes from the symmetry breaking induced by the tension because the GO has to bend to cover the ZnO QDs [19]. The D peak (1348 cm^{-1}) results from the K to K' mode of A1g dispersion. If the G band of the pristine GO is compared with the CS, a blue shift can be observed, indicating a distortion in its sp^2 hybridization on the GO surface [18].

The appearance of the D+G band (2706 cm^{-1}) is due to the increase in disorder in GO. Also, the overtone of the 2D peak (2690 cm^{-1}) increases in intensity due to the presence of a nucleus. In the case of ZnO QDs[19], there is a strong charge interaction or energy transfer between the nucleus and the GO layer.

At the same time, the presence of disorder can be calculated by the relationship between the defect disorder (D band) and the intensity of the graphitic system (G band), that is, the I_D/I_G ratio. As observed, the spectra predominate sp^2 sites, where the G peak is more pronounced than the D peak. The I_D/I_G ratio revealed a value of 0.90 for GO. The I_D/I_G ratio for the case of CS is 1.4; this change implies the addition of defects in the network in the ratio of GO and CS.

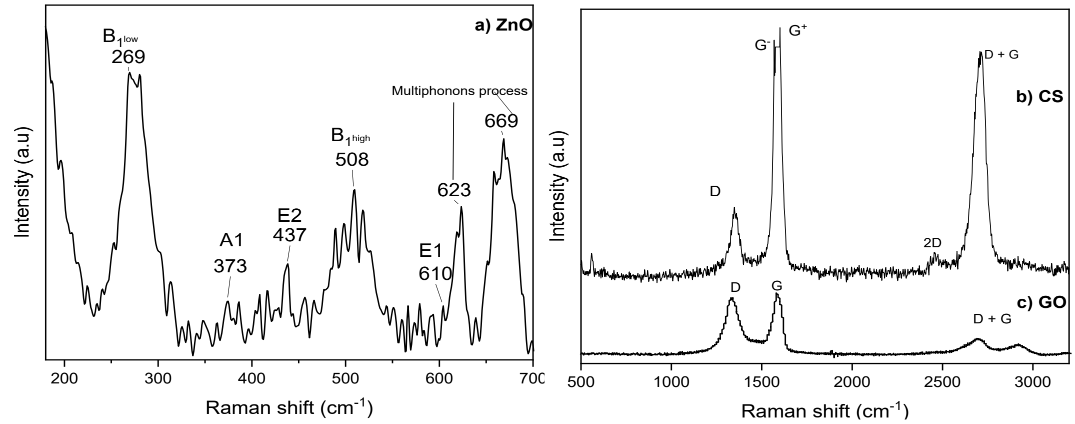

Fig. 3. Raman spectra of different nanomaterials a) ZnO, b) GO, and c) CS.

4.3. TEM

In Fig. 4a, a GO flake is shown being deformed with the LPE process synthesized with DMSO and EG, which shows a rolling up starting at the edges of the flake, which, in Fig. 4b, the development of surface deformation with the formation of "wrinkles" and the formation of spheres on the surface of the GO and with a more significant population at the edge of the flake is observed, the flake deformation procedure decreases the stability of the Van der Waals interaction, causing an increase in curvature, making the this shape less stable, appearing overlapping regions, which overcomes the energy barrier.

In Fig. 4c, the CS synthesis, is increasing the sonication times to guarantee the complete formation of ZnO-GO CS. Therefore, the ultrasound increases the shear and deformation forces on the GO flake and performs a rolling up and encapsulation. The average sizes of the CS are 8 nm, which is observed at an interplanar distance of 0.24 nm corresponding the GO layer covering the ZnO core.

The series of plane families of the shell is characteristic of ZnO, related to the hexagonal structure in a symmetric manner: (100), (110), and (200) as a function of the symmetric distances. Fig. 4d. GO, lacking a strict crystalline structure, can enhance the stability of ZnO and affect the ZnO planes interact with their surroundings [20].

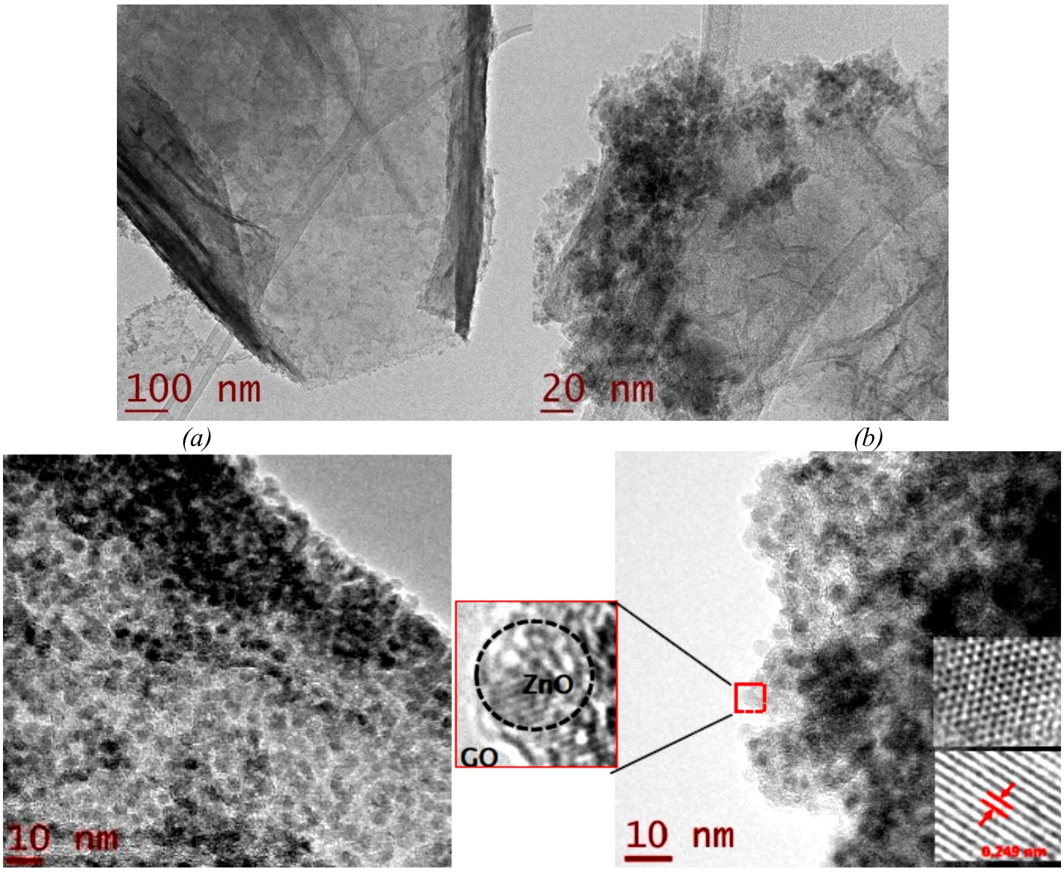

(a) (b)

(c) (d)

Fig. 4. TEM images of a layer rolling, b) layer with wrinkles and rolls in the edge, c) and d) CS of ZnO QDs-GO.

5. Conclusions

This study demonstrates that the ultrasonic synthesis method for preparing ZnO QDs-GO CS is a green chemistry method with factors such as solvents, surface modifiers and temperature. All this contributes to the GO sheet's deformation and flexibility and the ability to wrap the ZnO QDs homogeneously and stably against agglomeration. The results demonstrate that forming a hybrid material such as CS is possible and can be implemented in various optics, imaging, optoelectronics, or biomedicine applications.

Acknowledgements

The authors thankfully acknowledge the financial support of this work by the Instituto Politécnico Nacional through SIP-IPN projects 20242751 and 20241489. A.J. López Ramírez recognizes the CONAHCYT PhD scholarship. Also, the authors thank CNMN-IPN for its experimental support. The authors also would like to thank Henry Jankiewicz for the editing work and M. García Murillo for her assistance.

References

[1] V. Chiozzi, F. Rossi, Nov. 01, 2020, Royal Society of Chemistry; https://doi.org/10.1039/D0NA00411A

[2] A. Jana, E. Scheer, Langmuir, vol. 34, no. 4, pp. 1497-1505, Jan. 2018; https://doi.org/10.1021/acs.langmuir.7b02953

[3] E. Moyen, J. H. Kim, J. Kim, J. Jang, ACS Appl Nano Mater, vol. 3, no. 6, pp. 5203-5211, Jun. 2020; https://doi.org/10.1021/acsanm.0c00639

[4] Z. Jiang et al., Sep. 15, 2023, Elsevier Ltd.; https://doi.org/10.1016/j.jallcom.2023.170316

[5] D. Haranath, S. Sahai, A. G. Joshi, B. K. Gupta, V. Shanker, Nanotechnology, vol. 20, no. 42, 2009; https://doi.org/10.1088/0957-4484/20/42/425701

[6] L. Spanhel, M. A. Anderson, Semiconductor Clusters in the Sol-Gel Process: Quantized Aggregation, Gelation, and Crystal Growth in Concentrated ZnO Colloids, 1991; https://doi.org/10.1002/chin.199128252

[7] P. Singh, R. K. Singh, R. Kumar, RSC Adv, vol. 11, no. 4, pp. 2512-2545, Jan. 2021; https://doi.org/10.1039/D0RA08670C

[8] Y. R. Kumar, K. Deshmukh, K. K. Sadasivuni, S. K. K. Pasha, Jun. 23, 2020, Royal Society of Chemistry; https://doi.org/10.1039/D0RA03938A

[9] M. K. Rabchinskii, M. V Gudkov, D. Y. Stolyarova, Graphene Chemical Derivatives Synthesis and Applications: State-of-the-Art and Perspectives, 2022; https://doi.org/10.1002/9783527823963.ch1

[10] J. Gu et al., J Memb Sci, vol. 685, Nov. 2023; https://doi.org/10.1016/j.memsci.2023.121978

[11] A. R. S. Santha Kumar et al., Ultrasonics in polymer science: applications and challenges, Jul. 01, 2023, Elsevier Ltd.; https://doi.org/10.1016/j.pmatsci.2023.101113

[12] A. Ciesielski, P. Samorì, Jan. 07, 2014, Royal Society of Chemistry; https://doi.org/10.1039/C3CS60217F

[13] R. Narayan, S. O. Kim, Dec. 01, 2015, Korea Nano Technology Research Society; https://doi.org/10.1186/s40580-015-0050-x

[14] A. A. Moosa, M. S. Abed, Graphene preparation and graphite exfoliation, 2021, Tubitak; https://doi.org/10.3906/kim-2101-19

[15] J. Douda, C. R. González Vargas, E. V. Basiuk, A. I. Díaz Cano, J. A. Fuentes García, X. A. Hernández Contreras, Applied Nanoscience (Switzerland), vol. 9, no. 4, pp. 567-578, Jun. 2019; https://doi.org/10.1007/s13204-019-00956-z

[16] R. Zhang, P. G. Yin, N. Wang, L. Guo, Solid State Sci, vol. 11, no. 4, pp. 865-869, Apr. 2009; https://doi.org/10.1016/j.solidstatesciences.2008.10.016

[17] P. Shankar et al., Appl Surf Sci, vol. 531, Nov. 2020; https://doi.org/10.1016/j.apsusc.2020.147365

[18] P. Singh, R. K. Singh, R. Kumar, RSC Adv, vol. 11, no. 4, pp. 2512-2545, Jan. 2021; https://doi.org/10.1039/D0RA08670C

[19] S. S. P. Haghshenas, A. Nemati, R. Simchi, C. U. Kim, Ceram Int, vol. 45, no. 7, pp. 8945-8961, May 2019; https://doi.org/10.1016/j.ceramint.2019.01.226

[20] D. I. Son et al., Nat Nanotechnol, vol. 7, no. 7, pp. 465-471, 2012; https://doi.org/10.1038/nnano.2012.71